Increasing the Accuracy for a Piezo-Actuated Micro Manipulator for Industrial Robots using Model-Based Nonlinear Control [⋆]

Björn Olofsson [∗] **Olof Sörnmo** [∗] **Ulrich Schneider** [∗∗] **Marc Barho** [∗∗]
Anders Robertsson [∗] **Rolf Johansson** [∗]

[∗] *Department of Automatic Control, LTH, Lund University,*
SE–221 00 Lund, Sweden. E–mail: Bjorn.Olofsson@control.lth.se.
[∗∗] *Fraunhofer Institute for Manufacturing and Engineering, Nobelstraße 12,*
D–70569 Stuttgart, Germany.

Abstract: We consider the problem of modeling and control of the nonlinear dynamics of a micro manipulator, utilized for machining operations in combination with industrial robots. Position control of the micro manipulator is a challenging problem because of the actuation principle, which is based on piezo-actuators with inherent nonlinear behavior. The major nonlinearities in the manipulator are identified and explicitly modeled in this paper. Different model structures are outlined and subsequent identification experiments are performed and evaluated. The obtained models form the basis for a combined feedforward and feedback control scheme for accurate position control. Experimental results obtained with the developed control scheme are presented and discussed. We show that the accuracy of the controller is increased significantly with the proposed scheme, compared to a linear controller.

1. INTRODUCTION

As a result of the increased demand on cost-efficiency and flexibility in the manufacturing industry, industrial robots have emerged during the past decade as an appealing alternative to the dedicated machine-tools for performing high-accuracy machining operations, such as milling and grinding. Because of the significant process forces required during machining operations, joint flexibilities in combination with lack of measurements on the arm side of the robot, limit the achievable accuracy (Zhang et al., 2005). Consequently, deviations from the nominal path may occur during the machining operation.

To overcome the limitations of industrial robots when performing machining operations, a piezo-actuated micro manipulator has previously been developed (Puzik et al., 2009). The purpose of the developed micro manipulator is to compensate for path deviations, which the robot *per se* is unable to compensate for. The micro manipulator achieves this by stiff actuation, realized by piezo-actuators, combined with a mechanical design such that the bandwidth of the micro manipulator is significantly higher than that of the industrial robot. Following the concepts introduced by Sharon *et al.* (Sharon et al., 1993), the terms *micro manipulator* and *macro manipulator* will be used for the compensation mechanism and the robot, respectively.

We presented a prototype control scheme without explicit modeling of the nonlinear behavior of the piezo-actuators in (Olofsson et al., 2011), and a subsequent experimental evaluation in (Sörnmo et al., 2012). However, since the piezo-actuators in the micro manipulator are inherently nonlinear in their input-output dynamics, the performance of the control scheme, and hence the machining performance, can be increased by modeling the nonlinear dynamics and utilizing the models for feedforward control in the control scheme.

The main contribution of this paper is the development and application of a model-based control scheme for the nonlinear dynamics of the micro manipulator, as well as an analysis of the proposed feedforward controller based on describing functions. Furthermore, an experimental verification showing a significantly higher accuracy of the position control with the proposed control scheme, compared to a linear controller based on feedback, is presented.

This paper is organized as follows. In Sec. 2, the design of the micro manipulator is briefly reviewed. The theory for the nonlinear models of the piezo-actuators is given in Sec. 3, whereas the identified models and the control scheme for the nonlinear dynamics of the micro manipulator are presented in Sec. 4. Experimental results are provided in Sec. 5, and finally conclusions and aspects on future work are given in Sec. 6.

2. BACKGROUND

This section briefly reviews the mechanical design of the developed micro manipulator, which is displayed in Fig. 1. It is to be noted that the machining spindle is attached to the micro manipulator—*i.e.*, the robot is holding the workpiece—in the proposed experimental setup.

2.1 Mechanical design

The design of the micro manipulator is such that compensation is possible in a three-dimensional Cartesian coordinate system with axes x, y, and z, as shown in Fig. 1. Each axis is actuated by a piezo-actuator. Further, flexure elements between the actuators and the end-effector increase the compensation range of the micro manipulator. The gear ratio is approximately five in
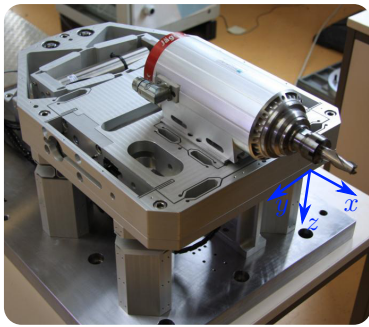
Fig. 1. Micro manipulator actuated by three piezo-actuators. The Cartesian coordinate system in blue indicates the actuation axes.
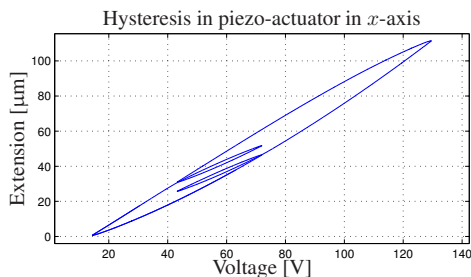

Fig. 2. Characterization of hysteresis in the x-axis of the micro manipulator in the case of a linear, alternatingly increasing and decreasing input with changing amplitude.

each axis, which results in a maximum compensation range of 0.5 mm in each Cartesian direction.

The displacement of the machining spindle along each of the axes is measured with a capacitive sensor, whereas the extensions of the piezo-actuators are measured with strain gauge sensors integrated into the actuators.

2.2 Nonlinear phenomena in the micro manipulator

During the initial dynamic characterization of the micro manipulator, it was noted that the nonlinear effects in the piezo-actuators are significantly influencing the positioning accuracy. The most apparent nonlinear dynamics were *hysteresis* and *creep* effects. The characteristics of the former phenomenon are shown in Fig. 2. The creep effect has been quantified for the different axes to approximately 0.02 µm/s.

Consequently, modeling of the nonlinear hysteresis effect is necessary in order to achieve accurate position control of the micro manipulator. Since the creep phenomenon exhibits significantly slower dynamics than the hysteresis, this effect can be handled without explicit modeling. Instead, feedback from the strain gauge sensors on the actuators is utilized. In particular, integral feedback from the control error is considered.

3. THEORY

Several approaches to modeling the hysteresis effect have been discussed in the literature. Three main categories of hysteresis models can be identified; approaches based on the *Preisach model* (Ge and Jouaneh, 1996; Lei et al., 2011), the *Prandtl-Ishlinskii model* (Al Janaideh et al., 2009; Krejci and Kuhnen, 2001; Sun and Yang, 2009) and *neural networks* (Hastie et al., 2008; Xu, 1993).
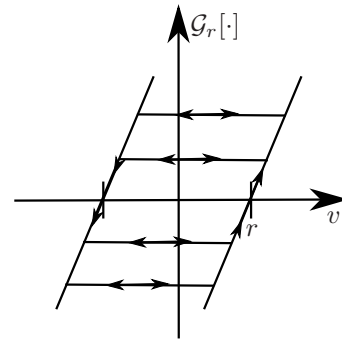

Fig. 3. Play operator $\mathcal{G}_r[\cdot]$ with symmetric threshold r.

In this paper, the focus will be on the Prandtl-Ishlinskii model and the neural network approach. Hence, the theoretical foundations of these approaches will be discussed next.

3.1 Prandtl-Ishlinskii model

The Prandtl-Ishlinskii model is based on the play operator $\mathcal{G}_r[\cdot]$ depicted in Fig. 3. Following (Brokate and Sprekels, 1996), a continuous function $v(t) \in \mathcal{C}[0, T]$, piecewise monotone in each of the subintervals

$$[t_i, t_{i+1}], \ 0 = t_0 < t_1 < \ldots < t_N = T \qquad (1)$$

is assumed as input. Hence, the play operator $\mathcal{G}_r[\cdot]$ can in each subinterval $[t_i, t_{i+1}]$, $i = 0, \ldots, N-1$, be written as

$$\mathcal{G}_r[v](t) = \max(v(t) - r, \min(v(t) + r, \mathcal{G}_r[v](t_i))),$$
$$t_i < t \leq t_{i+1} \quad (2)$$

with the initial value

$$\mathcal{G}_r[v](0) = \max(v(0) - r, \min(v(0) + r, 0)) \qquad (3)$$

Utilizing the definition of the play operator in (2), the Prandtl-Ishlinskii operator $\mathcal{H}[v](t)$ can be written as a superposition of play operators according to (Brokate and Sprekels, 1996)

$$\mathcal{H}_1[v](t) = \alpha v(t) + \int_0^R \rho(r)\mathcal{G}_r[v](t)\mathrm{d}r \qquad (4)$$

where $\rho(r)$ is a positive density function and α is a constant parameter.

The *generalized Prandtl-Ishlinskii operator* (Al Janaideh et al., 2009), is an extension of the standard Prandtl-Ishlinskii model (4) in that the input $v(t)$ is shaped with a continuous and strictly increasing function $\varphi(\cdot)$. The generalized Prandtl-Ishlinskii operator can be written as (Al Janaideh et al., 2009)

$$\mathcal{H}_2[v](t) = \alpha(\varphi \circ v)(t) + \int_0^R \rho(r)\mathcal{G}_r[\varphi \circ v](t)\mathrm{d}r \quad (5)$$

To the purpose of implementation, a finite-dimensional Prandtl-Ishlinskii operator is established by discretization of the integral. This results in the finite-dimensional Prandtl-Ishlinskii operator

$$y_k = \alpha\varphi(v_k) + \sum_{i=1}^n \rho(r_i)\bar{\mathcal{G}}_{r_i}[\varphi(v_k)] \qquad (6)$$

where $Y = \{y_k\}$ and $V = \{v_k\}$ are considered as discrete time-series and $\bar{\mathcal{G}}_{r_i}[\cdot]$ denotes the discretized play operator.

3.2 Inverse model based on Prandtl-Ishlinskii operator

The advantage of using the Prandtl-Ishlinskii operator for modeling of the hysteresis is that the analytic inverse of the
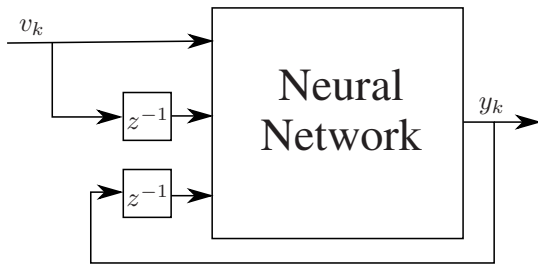
Fig. 4. Recurrent neural network with internal feedback from the output y_k. The neural network is to model the hysteresis of the piezo-actuators.

model (6) with a finite number of play operators exists. The inverse is given by, *e.g.*, (Al Janaideh et al., 2009),

$$v_k = \varphi^{-1}\left(\frac{1}{\alpha}y_k + \sum_{i=1}^{n}\hat{\rho}(\hat{r}_i)\bar{\mathcal{G}}_{\hat{r}_i}[y_k]\right) \qquad (7)$$

where

$$\hat{r}_i = \alpha r_i + \sum_{j=1}^{i-1}\rho(r_j)(r_i - r_j) \quad \text{and} \qquad (8)$$

$$\hat{\rho}(\hat{r}_i) = -\frac{\rho(r_i)}{\left(\alpha + \sum_{j=1}^{i}\rho(r_j)\right)\left(\alpha + \sum_{j=1}^{i-1}\rho(r_j)\right)} \qquad (9)$$

It is to be noted that the shaping function $\varphi(\cdot)$ is invertible, which follows from the assumptions on $\varphi(\cdot)$ to be continuous and strictly monotone.

3.3 Neural network approach

Another approach to modeling the hysteresis phenomenon is based on neural networks. In particular, neural networks with internal feedback from the output, referred to as *recurrent neural networks*, are of interest for modeling of the nonlinear hysteresis effect, since they capture the inherent memory effect.

Consequently, consider the recurrent neural network in Fig. 4, which has been used for modeling of hysteresis in, *e.g.*, (Xu, 1993). Define a discrete-time neural network with input

$$X_k = [v_k \ v_{k-1} \ y_{k-1}]^T \,, \qquad (10)$$

output $Y_k = y_k$, one hidden layer and M neurons, described at time k by the relations

$$Z_m = \sigma\left(\left(w_m^{(1)}\right)^T X_k + b_m^{(1)}\right), \ m = 1,\ldots,M \qquad (11)$$

$$Y_k = \sum_{m=1}^{M} w_m^{(2)} Z_m + b_m^{(2)} \qquad (12)$$

where $w_m^{(1)} \in \mathbb{R}^3$, $b_m^{(1)}, w_m^{(2)}, b_m^{(2)} \in \mathbb{R}$, and the activation function $\sigma(v) = 1/(1 + \exp(-v))$. After training of the network—*i.e.*, identification of the model parameters—with experimental input-output data, the network output represents the hysteresis model output.

3.4 Inverse hysteresis model based on neural network

To the purpose of feedforward control based on the nonlinear model of the hysteresis dynamics, a neural network can be utilized to model the inverse relation as well. By interpreting y_k as the input and v_k as the output, the inverse model can be established based on the recurrent neural network in Fig. 4.

4. RESULTS

Hysteresis models were identified based on experimental input-output data. Since it is desirable that the model represents the hysteresis for different frequencies of the input signal, an excitation signal containing frequencies in the range of interest was chosen. Accordingly, the input signal

$$v(t) = v_0 + \sum_{i=1}^{n} a_i \sin(\omega_i t) \qquad (13)$$

where v_0 is an offset and a_i and ω_i, $i = 1,\ldots,n$, are the amplitudes and frequencies of the sinusoids, was applied to the micro manipulator.

4.1 Models based on Prandtl-Ishlinskii operator

The model parameters were identified using nonlinear optimization. Introduce the notation p for the set of parameters to be identified. To the purpose of parameter identification, the following quadratic cost function is considered

$$J(p) = \sum_{i=1}^{N}\left(y_k - y_k^{(m)}\right)^2 \qquad (14)$$

where $y_1,\ldots,y_N$ is the identification data and $y_1^{(m)},\ldots,y_N^{(m)}$ is the corresponding model output. With the threshold values r_i parametrized in the parameter β according to $r_i = \beta i$ with $\beta > 0$, and the density function $\rho(r) = \gamma \exp(-\delta r)$ with $\gamma, \delta > 0$, several different models with n play operators were identified. In particular, the choice of the shaping function $\varphi(\cdot)$ is of importance in order to obtain good correspondence between experimental data and the model. The following shaping functions common in the literature were considered

$$\varphi_1(v) = c_1 v + c_2 \qquad (15)$$
$$\varphi_2(v) = c_3 \tanh(c_4 v + c_5) + c_6 \qquad (16)$$

where c_i, $i = 1,\ldots,6$, are model parameters to be identified. The selection criterion for the shaping function was the final cost $J(p^*)$, where p^* is the vector of optimal parameter values.

The output from the identified model of the hysteresis nonlinearity in the x-axis of the micro manipulator, with the shaping function $\varphi_2(v)$ in Eq. (16) and $n = 6$, is compared to the measurements from the experimental setup in Fig. 5. It is to be noted that the model exhibits a good fit to the experimental data and that the input-output relation for the input signal of choice is satisfactory. The corresponding models for the y- and z-axes are similar, and are therefore not presented here.

4.2 Models based on recurrent neural network

Hysteresis models based on the recurrent neural network were trained using the cost function in Eq. (14) and with stochastic initialization of the model parameters $\{b_m^{(1)}, b_m^{(2)}, w_m^{(1)}, w_m^{(2)}\}$, based on a normal distribution. A model for the x-axis nonlinearity with $M = 25$ neurons was found to result in similar performance as the previous Prandtl-Ishlinskii model. The model details are omitted here because of the limited space. Further, a neural network was trained for the inverse of the nonlinearity, which can be utilized to the purpose of feedforward control.

4.3 Scheme for position control

The control scheme depicted in Fig. 6 is proposed. In this scheme, each of the Cartesian axes of the micro manipulator is
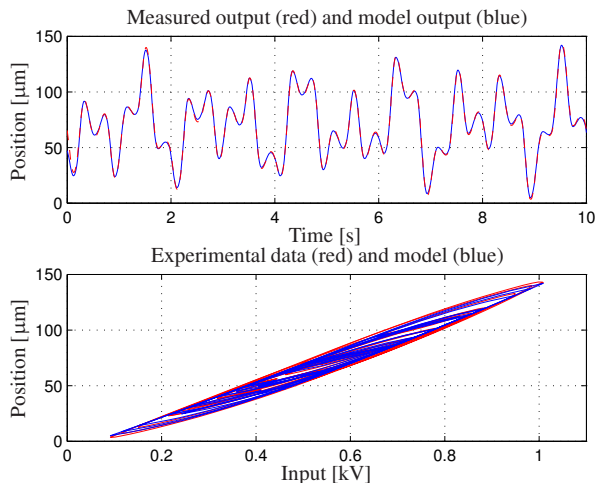
Fig. 5. Model based on Prandtl-Ishlinskii operator with output as function of time (upper panel) and output as function of input (lower panel).

considered separately—*i.e.*, possible cross couplings between the axes are neglected.

4.4 Inner control scheme for piezo-actuators

Based on the inverse of the previously identified models of the hysteresis nonlinearity in the micro manipulator, a combined feedforward and feedback control scheme is proposed. A feedforward controller alone is not sufficient, since unmodeled dynamics and parameter variations will degrade the performance significantly. Consequently, feedback from the strain gauge sensors attached to the piezo-actuators is necessary.

The feedforward controller is based on the inverse of the hysteresis nonlinearity in the micro manipulator. The inverse model is established for each Cartesian axis as described in Sec. 3; either from the model based on the Prandtl-Ishlinskii operator or training a neural network for the inverse function directly.

The feedback controller is chosen as a PID controller, whose control law is given by

$$u(t) = K\left[e(t) + \frac{1}{T_i}\int_0^t e(\tau)\mathrm{d}\tau + T_d\frac{\mathrm{d}e(t)}{\mathrm{d}t}\right] \quad (17)$$

where $u(t)$ is the control signal, $e(t)$ the control error, and K, T_i, and T_d are controller parameters. The D-part is essential, since it contributes with phase advance in the system. Furthermore, the D-part is lowpass-filtered in order to avoid amplification of high-frequency noise and the I-part is accompanied by an anti-windup scheme. The parameters of the PID controller should be chosen such that the gain is maximized, without causing instability of the closed-loop system, in order to reduce the effects of the nonlinearities in the piezo-actuators.

4.5 Outer control loop for micro manipulator position

With the inner piezo-actuator control loops closed, the linear dynamics of the micro manipulator is identified using *subspace-based* identification methods (Johansson, 1993). The position is controlled by a model-based *linear-quadratic Gaussian* (LQG) optimal controller (Åström and Wittenmark, 1997), where the states in the model of the linear dynamics are estimated using a *Kalman filter*. For further details regarding this controller, the reader is referred to (Olofsson et al., 2011).

4.6 Describing function analysis of the feedforward controller

In order to analyze the properties of the feedforward control based on the Prandtl-Ishlinskii operator, *describing function analysis*, see, *e.g.*, (Slotine and Li, 1991), is utilized. The describing function analysis is based on a Fourier series expansion of the output from the nonlinear model, with a sinusoidal input. Even though this is an approximate analysis in the frequency domain, it gives valuable information about the global behavior of the feedforward controller. The analysis can further be motivated by considering the fact that the linear dynamics of the micro manipulator is of lowpass character.

Consider the finite-dimensional inverse Prandtl-Ishlinskii model in (7). Further, assume continuous-time input and output. With the input $y(t) = y_0 + A\sin(\omega t)$, the first terms in the Fourier series expansion of the output are given by

$$v_0 = \frac{1}{2\pi}\int_0^{2\pi} f(y(t))\mathrm{d}(\omega t) \quad (18)$$

$$a_1 = \frac{1}{\pi}\int_0^{2\pi} f(y(t))\sin(\omega t)\mathrm{d}(\omega t) \quad (19)$$

$$b_1 = \frac{1}{\pi}\int_0^{2\pi} f(y(t))\cos(\omega t)\mathrm{d}(\omega t) , \quad (20)$$

where $f(\cdot)$ is the inverse hysteresis model mapping. The describing function $N(A)$ is defined based on the a_1 and b_1 coefficients as

$$N(A) = \frac{a_1 + ib_1}{A} \quad (21)$$

Introduce $\theta_i = \pi - \arcsin(1 - (2\hat{r}_i)/A)$ and

$$\Gamma_i = \begin{cases} 1 , & \text{if } A > \hat{r}_i \\ 0 , & \text{otherwise} \end{cases} \quad (22)$$

Assume that the shaping function $\varphi(v) = 1$ and $y_0 = 0$. It is straightforward to verify that $v_0 = 0$. The a_1 coefficient can, after simplification, be written as

$$\frac{a_1}{A} = \frac{1}{\alpha} + \frac{1}{\pi}\sum_{i=1}^{n}\hat{\rho}(\hat{r}_i)\Gamma_i\left\{\frac{3\pi}{2} + \frac{1}{2}\sin(2\theta_i)\right.$$
$$\left. + 2\left(\frac{2\hat{r}_i}{A} - 1\right)\cos(\theta_i) - \theta_i\right\} \quad (23)$$

A similar calculation for the b_1 coefficient gives

$$\frac{b_1}{A} = \frac{1}{\pi}\sum_{i=1}^{n}\hat{\rho}(\hat{r}_i)\Gamma_i\left\{-\frac{3}{2} + \frac{1}{2}\cos(2\theta_i)\right.$$
$$\left. + 2\left(1 - \frac{2\hat{r}_i}{A}\right)\sin(\theta_i)\right\} \quad (24)$$

Hence, the quantity $|N(A)| = \sqrt{a_1^2 + b_1^2}/A$ can be utilized as a measure of the amplitude-dependent gain.

The analysis can be extended to the case when $\varphi(\cdot)$ is a different function than the unity mapping and $y_0 \neq 0$. However, if the complexity of the shaping function is increased, calculation of the required integrals has to be performed using numerical quadrature. The describing function analysis is performed for the model presented in Fig. 5 with the shaping function $\varphi_2(v)$ in Eq. (16), whereby the offset and gain shown in Fig. 7 are obtained. In this analysis, the offset in the input signal has been chosen to $y_0 = 70$, which is in the middle of the working range of the piezo-actuators in the micro manipulator.

It is to be noted that no singularities are visible in the describing function within the amplitude range of interest, which is defined
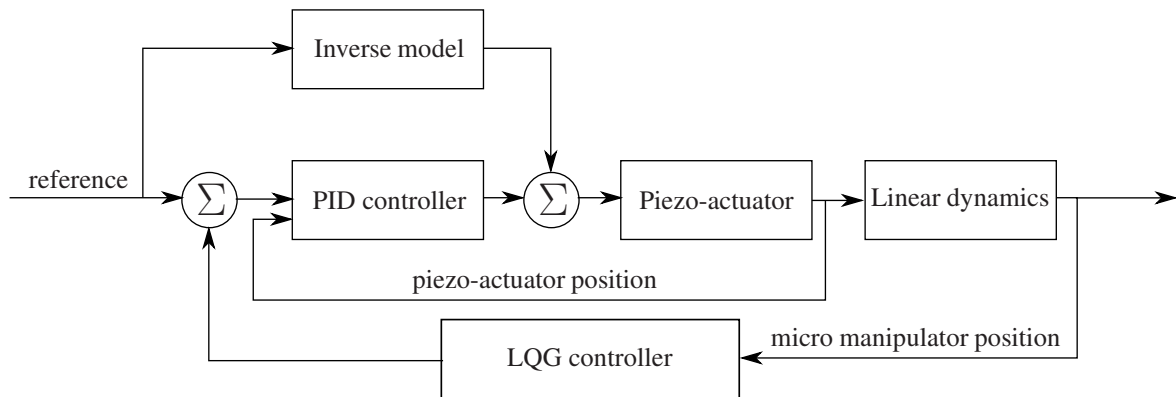
Fig. 6. Control scheme for position control of each axis of the micro manipulator. The reference signal is determined by a laser-based robot tracking system, measuring the deflections of the robot during the machining operation.
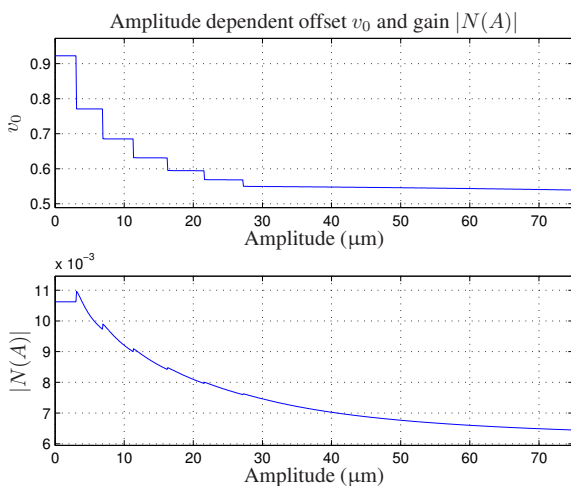

Fig. 7. Amplitude dependent offset v_0 and gain $|N(A)|$ for the hysteresis model in Fig. 5. The discrete character of the inverse model is clearly visible in the plots, where the stairs correspond to the threshold values $\hat{r}_i$, $i = 1, \dots, n$.
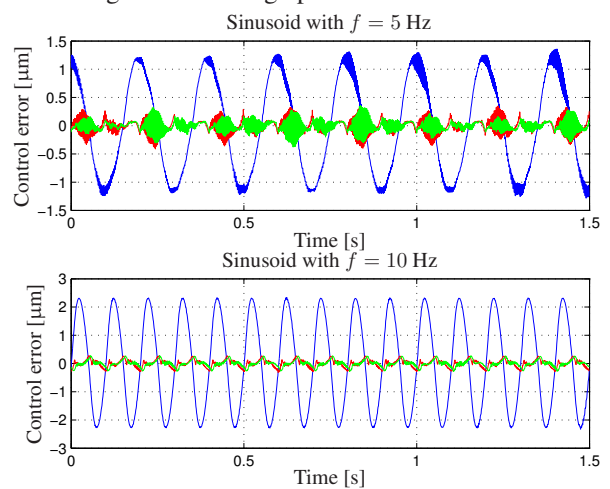

Fig. 8. Experimental control error for PID controller (blue), Prandtl-Ishlinskii model with affine shaping function (red) and Prandtl-Ishlinskii model with tanh shaping function (green), all with sinusoidal reference signal with frequencies 5 Hz (upper panel) and 10 Hz (lower panel).

by the working range of the micro manipulator. Hence, the describing function analysis indicates stability of the feedforward control scheme based on the inverse Prandtl-Ishlinskii model.

5. EXPERIMENTAL RESULTS

To the purpose of experimental verification, the feedforward controller based on the Prandtl-Ishlinskii operator, was implemented and tested on the experimental setup.

5.1 Experimental setup

The micro manipulator was interfaced *via* a dSPACE DS1103 system, where the sensor signals were read and the actuator signals were written. The control scheme was implemented in MATLAB Simulink, and then translated to C-code and compiled. The controller was installed in the dSPACE system and executed at a sampling frequency of 10 kHz.

5.2 Experimental verification of control scheme

The x-axis of the micro manipulator was chosen for evaluation of the proposed control scheme for the piezo-actuators. The results for the other axes are similar, and are therefore not presented here. The reference signals were of the format

$$v(t) = v_0 + A\sin(2\pi f t) \qquad (25)$$

where the frequency f was chosen to 1, 5, and 10 Hz based on the frequency range of interest for the application. The amplitude and offset, measured on the actuator side, were chosen to $A = 30$ μm and $v_0 = 70$ μm, respectively, which means that the major part of the working range of the actuator is covered. The evaluation was performed with the following configurations of the position controller for the piezo-actuator

A. Pure feedback control using PID control.
B. PID controller combined with feedforward control based on the Prandtl-Ishlinskii model with the affine shaping function $\varphi_1(\cdot)$ in Eq. (15).
C. PID controller combined with Prandtl-Ishlinskii model with tanh shaping function $\varphi_2(\cdot)$ in Eq. (16).

Further, for reasons of comparability, the tuning of the PID controller was identical in the different configurations. As a measure of the control accuracy, the control error was considered. The control errors for the experiments performed on the setup, with the controller configurations and reference signals discussed in the previous paragraph, are displayed in Fig. 8. The corresponding input-output behavior is displayed in Fig. 9. Furthermore, the maximum error e_m as well as the standard deviation σ_e of the control error are shown in Table 1 for the different reference signals.
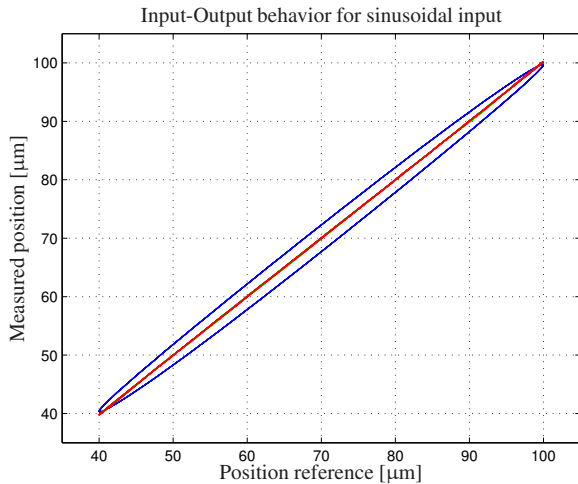
Fig. 9. Experimental input-output behavior for PID controller (blue), Prandtl-Ishlinskii model with affine shaping function (red) and Prandtl-Ishlinskii model with $\tanh$ shaping function (green), all with sinusoidal reference signal with frequency 10 Hz.

Table 1. Maximum error e_m and standard deviation σ_e of control error.

Maximum error e_m [μm]

Input freq. [Hz]	Configuration		
	A	B	C
1	0.829	0.505	0.525
5	2.65	0.823	0.739
10	4.68	0.592	0.590

Standard deviation σ_e [μm]

Input freq. [Hz]	Configuration		
	A	B	C
1	0.174	0.0632	0.0629
5	0.835	0.125	0.106
10	1.63	0.131	0.118

6. CONCLUSIONS AND FUTURE WORK

This paper has considered the problem of increasing the positioning accuracy of a piezo-actuated micro manipulator for industrial robots by utilizing model-based nonlinear control. Explicit nonlinear models of the major nonlinearity in the manipulator—*i.e.*, the hysteresis phenomenon—were identified based on experimental data. Two model categories were considered; models based on the Prandtl-Ishlinskii operator and models based on recurrent neural networks. A subsequent control scheme was proposed, where the properties of the feedforward controller was analyzed using describing functions.

In an experimental verification, the identified models were utilized in a control scheme combining feedforward and feedback. Experimental results showed that the proposed control scheme for position control of the micro manipulator increases the accuracy significantly for reference signals with different frequencies, compared to a linear controller. For a sinusoidal input with frequency 10 Hz, the maximum and the standard deviation of the control error are reduced by a factor of approximately ten.

As future work, other model structures for the hysteresis nonlinearity will be considered. Further, accelerometer sensor data will be utilized in an extension of the control scheme.

REFERENCES

Al Janaideh, M., Feng, Y., Rakheja, S., Su, C.Y., and Alain Rabbath, C. (2009). Hysteresis compensation for smart actuators using inverse generalized Prandtl-Ishlinskii model. In *Proc. Am. Control Conf. (ACC)*, 307–312. St. Louis, MO.

Åström, K.J. and Wittenmark, B. (1997). *Computer-Controlled Systems*. Prentice Hall, Englewood Cliffs, NJ.

Brokate, M. and Sprekels, J. (1996). *Hysteresis and Phase Transitions*. Springer-Verlag, New York.

Ge, P. and Jouaneh, M. (1996). Tracking control of a piezo-ceramic actuator. *IEEE Trans. Control Syst. Technol.*, 4(3), 209–216.

Hastie, T., Tibshirani, R., and Friedman, J. (2008). *The Elements of Statistical Learning*. Springer-Verlag, New York.

Johansson, R. (1993). *System Modeling and Identification*. Prentice Hall, Englewood Cliffs, NJ.

Krejci, P. and Kuhnen, K. (2001). Inverse control of systems with hysteresis and creep. In *IEE Proc. Control Theory and Applications*, volume 148, 185–192.

Lei, L., Tan, K.K., Huang, S., and H, L.T. (2011). Online parameter estimation and compensation of Preisach hysteresis by SVD updating. In *Proc. 18th IFAC World Congress*, 5249–5254. Milano, Italy.

Olofsson, B., Sörnmo, O., Schneider, U., Robertsson, A., Puzik, A., and Johansson, R. (2011). Modeling and control of a piezo-actuated high-dynamic compensation mechanism for industrial robots. In *Proc. IEEE/RSJ Int. Conf. on Intelligent Robots and Systems (IROS)*, 4704–4709. San Francisco, CA.

Puzik, A., Pott, A., Meyer, C., and Verl, A. (2009). Industrial robots for machining processes in combination with an additional actuation mechanism for error compensation. In *7th Int. Conf. on Manufacturing Research (ICMR)*. University of Warwick, United Kingdom.

Sharon, A., Hogan, N., and Hardt, D.E. (1993). The macro/micro manipulator: An improved architecture for robot control. *Robotics & Computer-Integrated Manufacturing*, 10(3), 209–222.

Slotine, J.J.E. and Li, W. (1991). *Applied Nonlinear Control*. Prentice Hall, Upper Saddle River, NJ.

Sörnmo, O., Olofsson, B., Schneider, U., Robertsson, A., and Johansson, R. (2012). Increasing the milling accuracy for industrial robots using a piezo-actuated high-dynamic micro manipulator. In *Proc. IEEE/ASME Int. Conf. on Adv. Intelligent Mechatronics (AIM)*. Kaohsiung, Taiwan. *Accepted for publication*.

Sun, Y. and Yang, B. (2009). Compensation of hysteresis nonlinearity for the piezoelectric actuators. In *Proc. 3rd IEEE Int. Conf. on Computer Science and Information Technol. (ICCSIT)*, 307–312. St. Louis, MO.

Xu, J.H. (1993). Neural network control of a piezo tool positioner. In *Proc. Canadian Conf. on Electrical and Computer Engineering*, 333–336. Vancouver, Canada.

Zhang, H., Wang, J., Zhang, G., Gan, Z., Pan, Z., Cui, H., and Zhu, Z. (2005). Machining with flexible manipulator: toward improving robotic machining performance. In *IEEE/ASME Int. Conf. on Adv. Intelligent Mechatronics (AIM)*, 1127–1132. Monterey, CA.